View metadata, citation and similar papers at core.ac.uk

brought to you by CORE

provided by University of Strathclyde Institutional Repository

Strathprints Institutional Repository

Michala, A. L. and Barltrop, N. and Amirafshari, P. and Lazakis, I. and Theotokatos, G. (2016) An intelligent system for vessels structural reliability evaluation. In: International Conference on Maritime Safety and Operations. University of Strathclyde Publishing, Glasgow, pp. 171-179. ISBN 9781909522169 ,

This version is available at http://strathprints.strath.ac.uk/58434/

Strathprints is designed to allow users to access the research output of the University of Strathclyde. Unless otherwise explicitly stated on the manuscript, Copyright © and Moral Rights for the papers on this site are retained by the individual authors and/or other copyright owners. Please check the manuscript for details of any other licences that may have been applied. You may not engage in further distribution of the material for any profitmaking activities or any commercial gain. You may freely distribute both the url (http://strathprints.strath.ac.uk/) and the content of this paper for research or private study, educational, or not-for-profit purposes without prior permission or charge.

Any correspondence concerning this service should be sent to Strathprints administrator: strathprints@strath.ac.uk

An intelligent system for vessel structural reliability evaluation

A.L. Michala, N. Barltrop, P. Amirafshari, I. Lazakis & G. Theotokatos
Department of Naval Architecture, Ocean & Marine Engineering, University of Strathclyde, Glasgow, UK

ABSTRACT: An intelligent system is proposed within INCASS (Inspection Capabilities for Enhanced Ship Safety) project for evaluating ship structural reliability and assisting in fatigue damage and structure response assessment. The system combines hydrodynamic, finite element and structural reliability models.. The hydrodynamic analysis model is not discussed in this paper. The finite element model input is a mesh for the midship part of the vessel. Finally, the in-house structural reliability model input is the calculated output of the previous model as well as models for estimating crack development and propagation, corrosion growth and fatigue loading. The output includes the probability of failure for all the investigated components versus time which can be used to assess safe operation through the developed decision support software. The database can receive information from various sources including inspection and robotic systems data. The case study of a capsize bulk carrier the presents structural evaluation process.

1 INTRODUCTION

Ships and offshore structures degrade through their service life due to their exposure to environmental loads, harsh and corrosive marine environment, and design and fabrication imperfections. Due to inherent nature of uncertainties associated with degrading variables, estimation of these degradations prior to service of the structure suffers from significant lack of precision. Design of such structure by taking into account of high margin of safety would lead to non-cost-effective design and would not be feasible; hence these structures are designed under the assumption that sufficient inspection will be carried out during the service. Inspection and voyage data are collected during the life of the structure and be can be used to optimize inspection planning by defining improved inspection interval in addition to targeting the locations within the structure which possess higher probability of failure. In this work failure probability of the crack prone components of a bulk carrier are studied under the light of Bayesian updating methods, which makes use of inspection data by updating failure probabilities according to collected data see Figure 1.

1.1 Framework

Within the INCASS framework (INCASS 2014a & 2014b) the program uses hydrodynamic/static analysis and finite element data output in conjunction with historical data to estimate component structural reliability of ships illustrated in Figure 2.

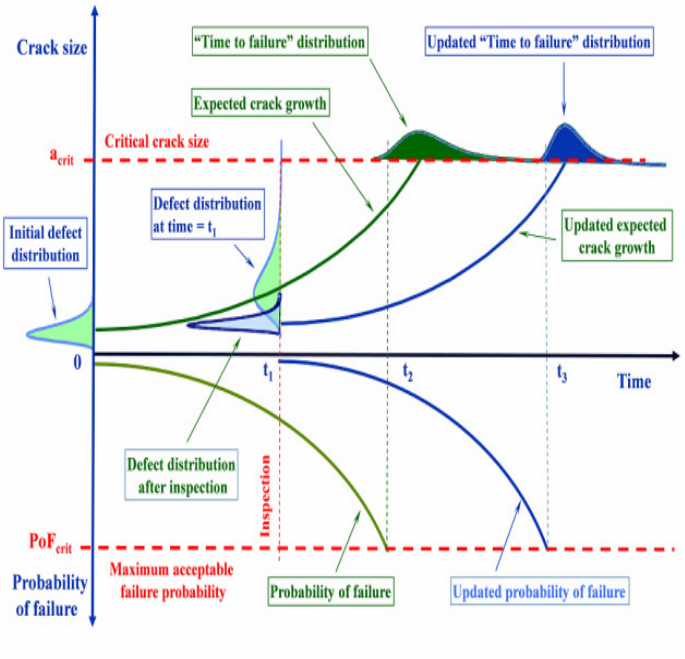

Figure 1 Schematic illustration of crack probability of fatigue failure before and after an inspection (DNV 2015)

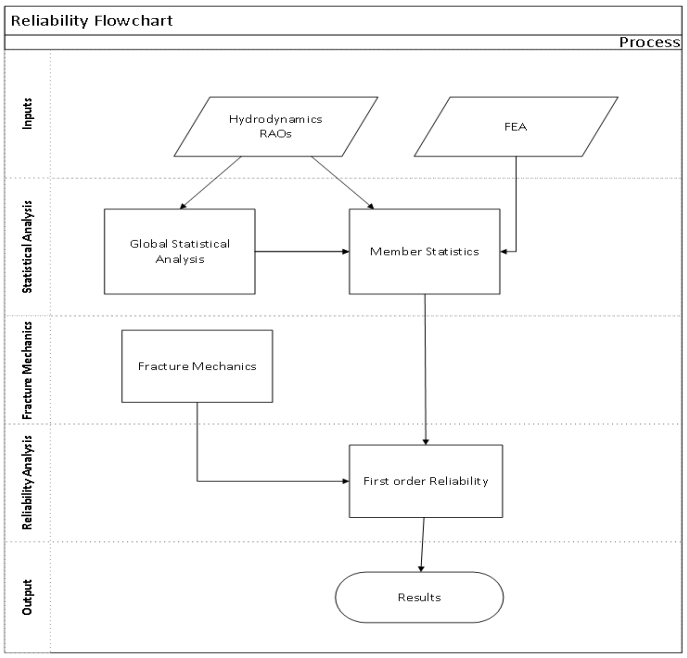

Figure 2 Program's work flow and relationship

2 FINITE ELEMENT ANALYSIS

For the purpose of structural analysis FEA analysis has been performed to calculate structural responses of the ship at component given in Table 1. These responses allow us to incorporate structural forces and in turn stresses which affect crack growth. Output results from FEA are transformed into probability distribution function by means of statistical analysis, and used in reliability analysis (INCASS 2014c). These structural responses are calculated for stiffeners and the panel connected to them shown in Figure 3.

Table 1 Structural response at component level.

Data	Description
N_x	Member Axial Force/m
N_y	Member transverse in plate-plane/m
N_{xy}	Member in plate-plane shear/m
N_{zx}	Member out of plate-plane shear force/m
M_y	Member stiffener moment/m
P	Member pressure force/m

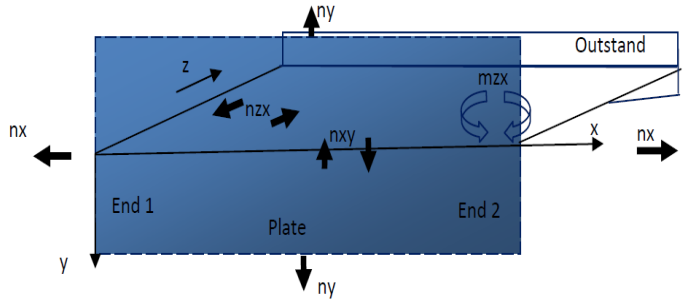

Figure 3 Representation of stiffeners, the underlying plate and corresponding forces

2.1 Modeling Components

The following components are modelled:1 All the plantings including outer and inner shell, main web frames and girders.2 All the bulkhead plantings and web frames are modelled with their actual dimensions and properties All longitudinal and transverse stiffeners of Inner and outer bottom, hopper tank side shell upper tanks and deck are modelled.3 In order to reduce the intensity of computation time, the stiffeners that are responsible to mitigate the local web buckling of girders and the respective web frames are not modelled.

2.2 Extent of model

To keep the model computational time reasonable, two adjacent holds at the midship area of the vessel were modelled, specifically, the holds four and five. In addition the relevant boundary conditions were set so that the modelled area behaves as the actual ship.

Each hold includes four main webs at top tanks not taking into account web frames at bulkhead locations. In this developed model, the transverse bulkhead between holds No. 4 and 5 along three main webs from each neighboring hold have been modelled, to achieve model symmetry and ensure that the perpendicular plains remain right after deformation. Hence the final model extends from the transverse frame 178 at aft to frame 214 (Fig 4).

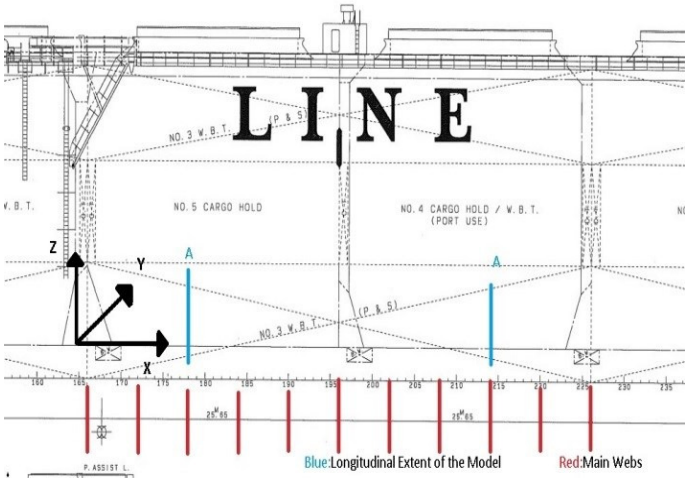

Figure 4 Longitudinal extent of the ship

2.3 Boundary conditions

Two sets of boundary conditions have been applied covering the cases of global responses and local responses, respectively.

Two remote points at aft and fore of the model, approximately at the same location of hull girder centroid have been defined; these two points are used to apply unit displacements for the case of global response, and to constrain nodes of outmost

aft and fore for the case of local responses as sown in Figure 5.

For the propos of global boundary conditions, the points at the top and bottom of the bulkhead perpendicular to the center line are constrained against displacement along X and Y. Two lines of nodes on port and aft of the side shell at the region where the bulkhead joins the side shell are constrained against displacement along Z axis.

With regards to local boundary conditions, all nodes at aft and fore of the model are constrained against displacement along X and Y axis. Two linear forces acting at side shells at bulkhead area equal to total force acting along Z axis are applied to fulfil support condition along Z axis. A minimum Z constrained condition on top of the bulkhead is defined to satisfy the stability of FE mathematical solution. The reaction force at this support after the analysis should be equal to zero.

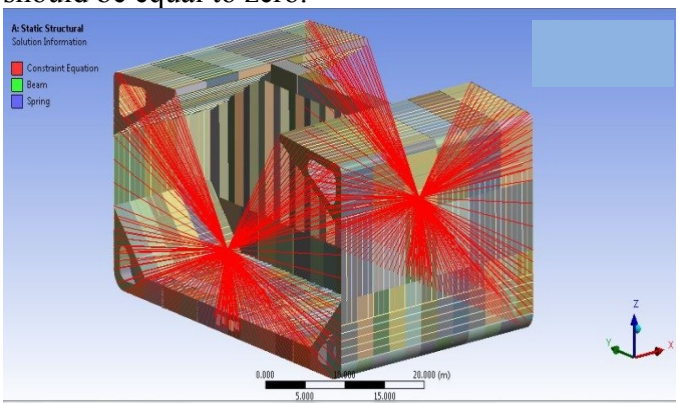

Figure 5 Definition of remote points at aft and fort of the model

2.4 Loading conditions

Eight loading conditions that are essential for reliability analysis are applied to the modelled structure. These can be categorized to two types, namely: Global loading conditions and Local loading conditions as reported in Table 2.

Table 3 Loading condition.

Loading Type	Local Effect
Load Case	External Water Pressure Internal Cargo Load Extreme Wave Pressure Fatigue Wave Pressure Slap Wave

2.5 Analysis

Linear static Analysis has been performed for each loading and boundary condition.

2.6 Typical results

Various results were derived from FE model analysis; however those that are relevant to the reliability module are stiffener forces and will be presented in this report. Figure 6 shows typical results for one longitudinal stiffener, and in specific the axial force along the length of the stiffener, for different load conditions. Figure 7 and Figure 8 show contour plots of axial force on stiffeners and Von Misses stress, respectively under fatigue wave pressure load.

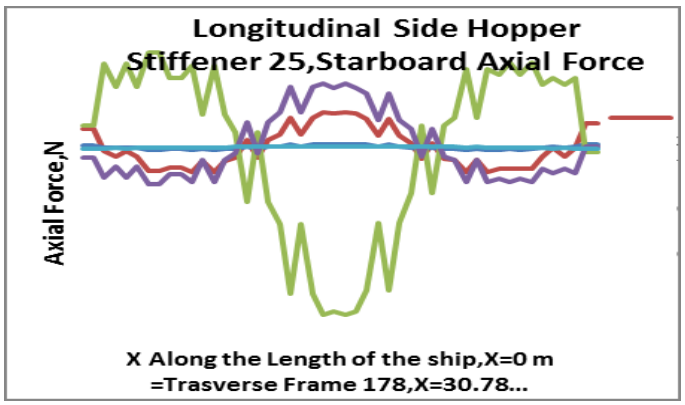

Figure 6 Longitudinal side hopper stiffener 25, starboard axial force.

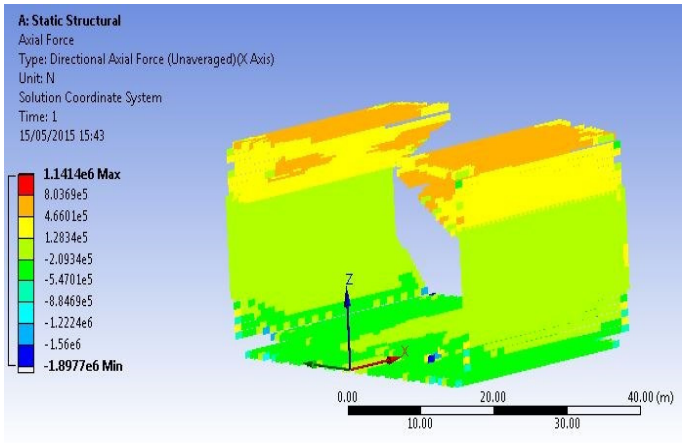

Figure 7 Axial force contour plot of longitudinal stiffeners fatigue wave pressure

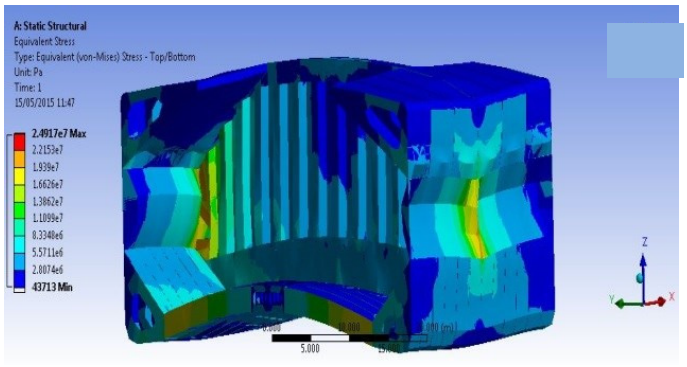

Figure 8 Equivalent stress plot under fatigue wave pressure load

2.7 Outputs

FE model results are exported from ANSYS to excel as shown in Figure 9 and subsequently read through using the Mathcad software so that the relevant results are provided as input to reliability code.

	Node Nun	X Locatior	Y Location	Z Location	Element N	Directional Axial Force (N)
2	371	0	-23	1.95	15585	-2257.1
3	375	1.2825	-23	1.95	15585	-2257.1
4	375	1.2825	-23	1.95	15586	-1701.3
5	55	2.565	-23	1.95	15564	-917.79
6	55	2.565	-23	1.95	15586	-1701.3
7	356	3.8475	-23	1.95	15564	-917.79
8	356	3.8475	-23	1.95	15565	-494.81
9	355	5.13	-23	1.95	15565	-494.81
10	355	5.13	-23	1.95	16510	-151.65
11	1350	6.4125	-23	1.95	16510	-151.65
12	1350	6.4125	-23	1.95	16511	125.79

Figure 9 FEA output to reliability code

3 STATISTICAL ANALYSIS

Reliability analysis evaluates the probability of structural failure by determining whether the limit-state functions are exceeded. However, reliability analysis is not limited to calculation of the probability of failure. Evaluation of various statistical properties, such as probability distribution functions and confidence intervals of structural responses, plays an important role in reliability analysis.

3.1 Weibull distribution

The Weibull distribution also referred to as the Type III extreme value distribution, is well suited for describing the weakest link phenomena, or a situation where there are competing flaws contributing to failure. It is often used to describe fatigue, fracture of brittle materials, and strength in composites.

The probability density function (of the two parameter version) is presented in Equation 1.

$$f_x(x) = \frac{\alpha\, x^{\alpha-1}}{\beta^{\alpha}} exp\left[-\left(\frac{x}{\beta}\right)^{\alpha}\right] \quad x \geq 0, \alpha > 0, \beta > 0 \qquad (1)$$

The CDF is presented in Equation 2.

$$F_x(x) = 1 - exp\left[-\left(\frac{x}{\beta}\right)^{\alpha}\right] \quad x > 0 \qquad (2)$$

3.2 Weibull distribution results

Global response amplitude operators of bulk carrier are presented below in terms of Weibull distribution for five nodes along the length of the ship (Figs 10, 11, 12).

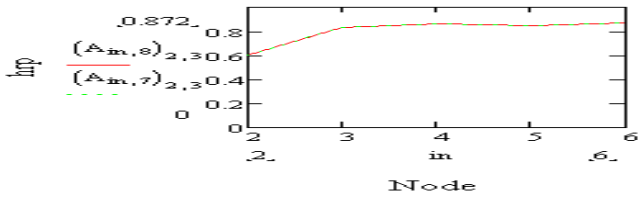

Figure 10 Global Weibull distribution of Water elevation at Port side and Starboard

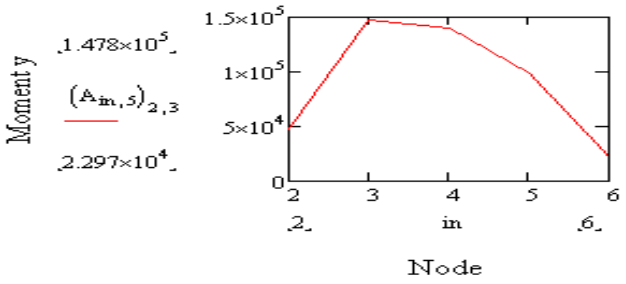

Figure 11 Global Weibull distribution of My

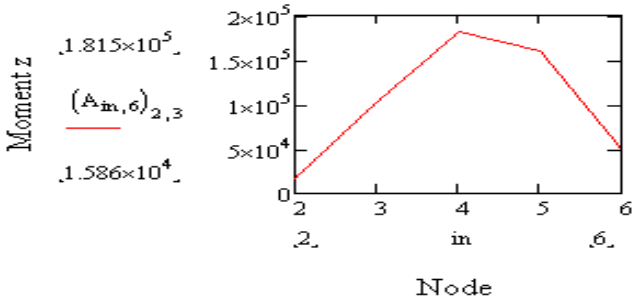

Figure 12 Global Weibull distribution of Mz

4 FRACTURE MECHANICS

Fatigue of welded connections consists of a fatigue initiation phase, a crack growth phase and a final fracture (phase). The fatigue test results from laboratory testing of welded connections include the cycles due to fatigue crack initiation and the following crack growth until failure. Most of the fatigue life in welded structures is associated with fatigue crack growth. In this document crack growth is assumed to occur from small (somewhat fictitiously small) initial cracks sizes such that a similar fatigue life is calculated by fracture mechanics as that of S-N test data.

The stress condition at a cracked region can be described by the concept of stress intensity factors. The general expression for the stress intensity factor describing the stress condition at crack tip region in a body with far field stress normal to the crack 2a is presented in Equation 3.

$$K_g = \sigma Y \sqrt{a\pi} \qquad (3)$$

In Equation 3 σ is the remote stress as indicated in the half crack length for the considered internal crack; a is the crack depth for edge cracks and Y is the geometry function. This function is equal 1.0 for a small crack in an infinite body. Otherwise it is a function of geometry that normally is larger than 1.0 (under tension load; may be less for bending).

Ships contain complicated details with sharp corners. Conventional crack growth and fracture analysis is too time-consuming. Hence, Assessment of crack growth at sharp corner based on "length scale": *ae* is employed leading to Equation 4 as demonstrated in Figures 13 to 14 and σ is the stress

with respect to distance from corner calculated through *ae* method (Equation 5).

$$K = \sigma Y \sqrt{\pi |a + ae|} \tag{4}$$

$$\sigma = \frac{\sigma_0 \sqrt{\pi} a s^p}{\sqrt{2\pi} x^p} \tag{5}$$

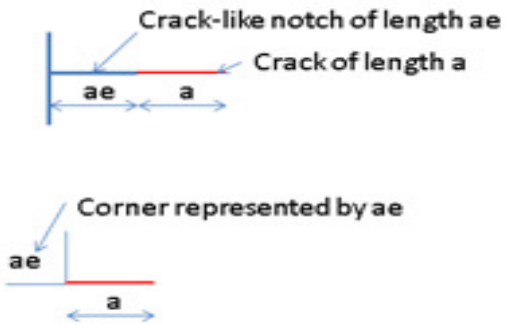

Figure 13 ae value as additional crack length (Barltrop 2014)

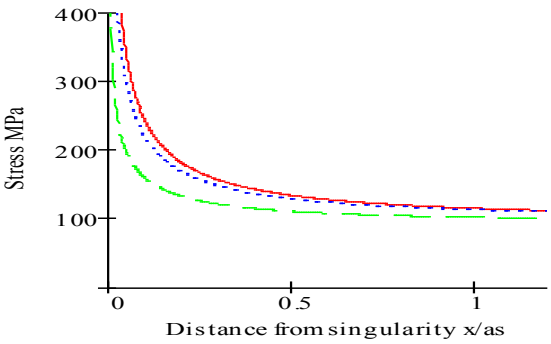

Figure 14 Stress with respect to distance from corner calculated through ae method (Barltrop 2014)

This Allows estimation of SCF and SIF (K) from dimensions, without requiring finite element analysis. For small cracks in corners the corner looks like an extra crack depth.

5 STRUCTURAL RELIABILITY ANALYSIS

When a structure (or part of a structure) exceeds a specific limit, the structure (or part of the structure) is unable to perform as required, and then the specific limit is called a limit-state. The structure will be considered unreliable if the failure probability of the structure limit-state exceeds the required value. For most structures, the limit-state can be divided into two categories: Ultimate limit-states are related to a structural collapse of part or all of the structure. Examples of the most common ultimate limit-states are corrosion, fatigue, deterioration, fire, plastic mechanism, progressive collapse, fracture, etc. Such a limit-state should have a very low probability of occurrence, since it may risk the loss of life and major financial losses. The limit-state function, *g(x)* , and probability of failure, *P(f)* , can be defined by Equation 6 and 7.

$$g(x) = R(x) - S(X) \tag{6}$$

$$P(f) = P[g(.) < 0] \tag{7}$$

where *R* is the resistance and *S* is the loading of the system. Both *R(x)* and *S(x)* are functions of random variables *X*. The notation $g(x) < 0$ denotes the failure region. Likewise, $g(x) = 0$ and $g(x) > 0$ indicate the failure surface and safe region, respectively.

The mean and standard deviation of the limit-state, *g(x)*, can be determined from the elementary definition of the mean and variance. The mean of *g(x)* is deducted through Equation 8.

$$\mu_g = \mu_R - \mu_S \tag{8}$$

where, μ_R and μ_S are the means of *R* and *S*, respectively. And the standard deviation of *g(x)* is

$$\sigma_g = \sqrt{\sigma_R^2 + \sigma_S^2 - 2\rho_{RS}\sigma_R}\sigma_S \tag{9}$$

where, ρ_{RS} is the correlation coefficient between *R* and *S*, and σ_R and σ_S are the standard deviations of *R* and *S*, respectively. The safety index or reliability index, β, is defined as:

$$\beta = \frac{\mu_g}{\sigma_g} = \frac{\mu_R - \mu_S}{\sqrt{\sigma_R^2 + \sigma_S^2 - 2\rho_{RS}\sigma_R\sigma_S}} \tag{10}$$

The shaded area of Figure 15 identifies the probability of failure. For a special case, the resistance, *R*, and loading, *S*, are assumed to be normally distributed and uncorrelated. The limit-state function is also normally distributed, since *g(x)* is a linear function of *R* and *S*. Thus, the probability density function of the limit-state function in this case is:

$$f(g) = \frac{1}{\sigma_g \sqrt{2\pi}} exp\left[-\frac{1}{2}\left(\frac{g-\mu_g}{\sigma_g}\right)^2\right] \tag{11}$$

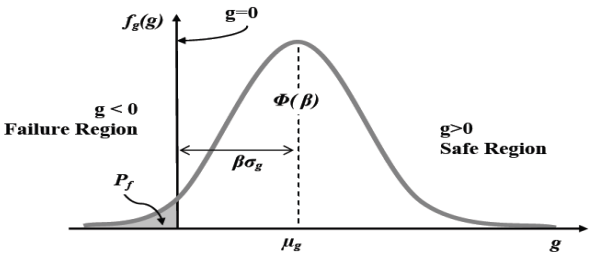

Figure 15 Failure probability (Choi, Grandhi, and Canfield 2006)

The probability of failure is presented in Equation 12 (Choi, Grandhi, and Canfield 2006)

$$P_f = \int_{-\infty}^{0} f_g(g)dg \tag{12}$$

In this paper one of the longitudinal stiffeners at Hooper tank has been studied (Fig 16-20). In this study failure probabilities associated with crack at relevant connection are studied and are presented in Figure 21 and Figure 22.

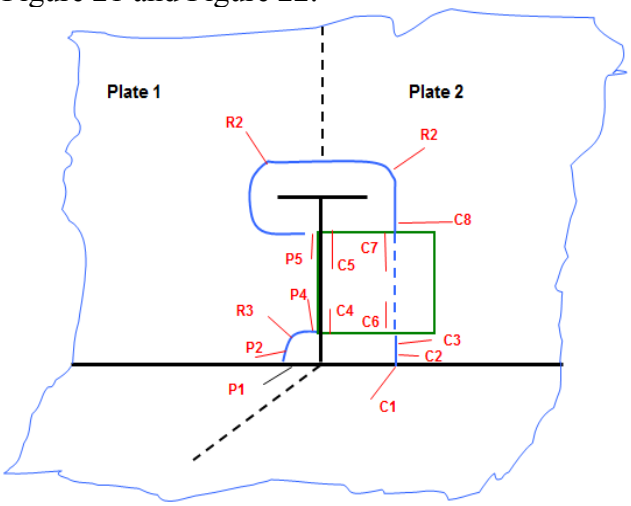

Figure 16 Representative results for Crack C1

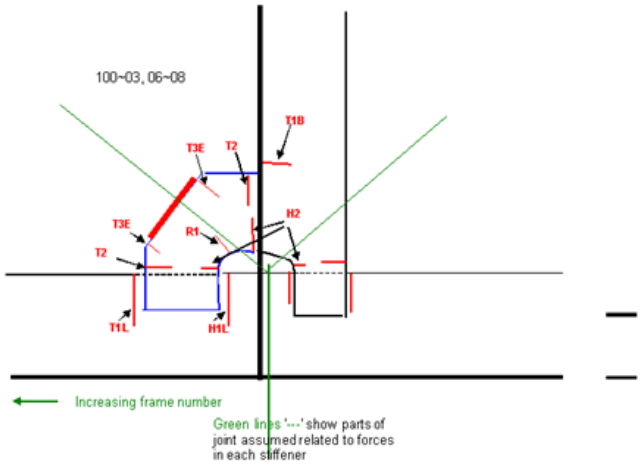

Figure 17 Possible crack growth, side view

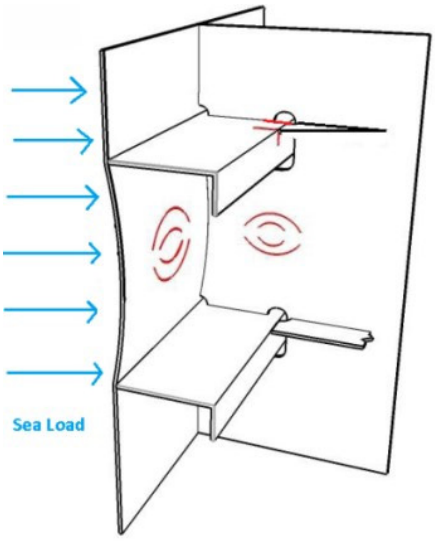

Figure 18 See load imposed on the connection.

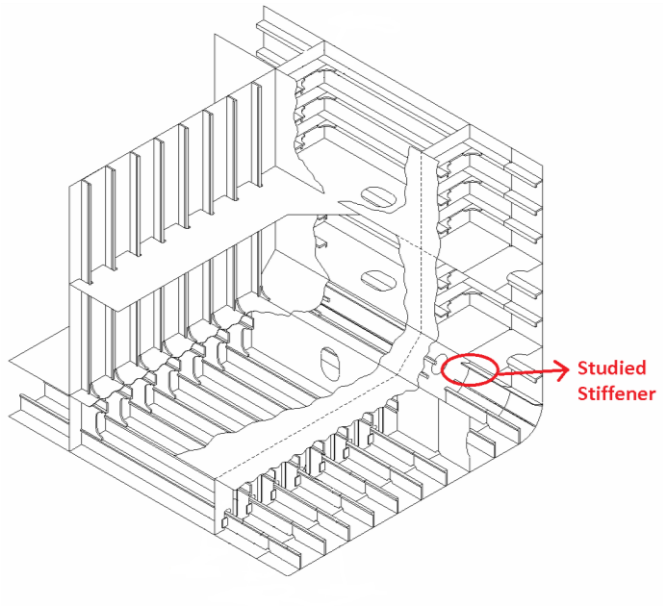

Figure 19 Schematic view of studied longitudinal stiffener

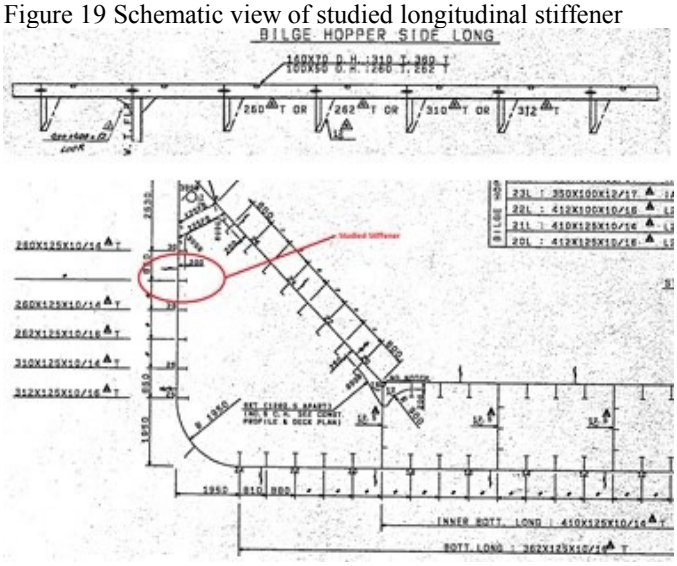

Figure 20 Studied Stiffener

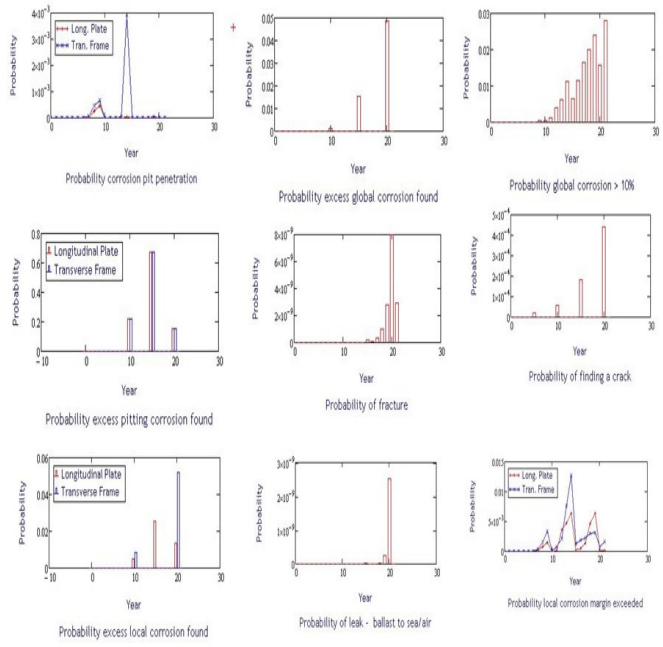

Figure 21 representative results for Crack C1

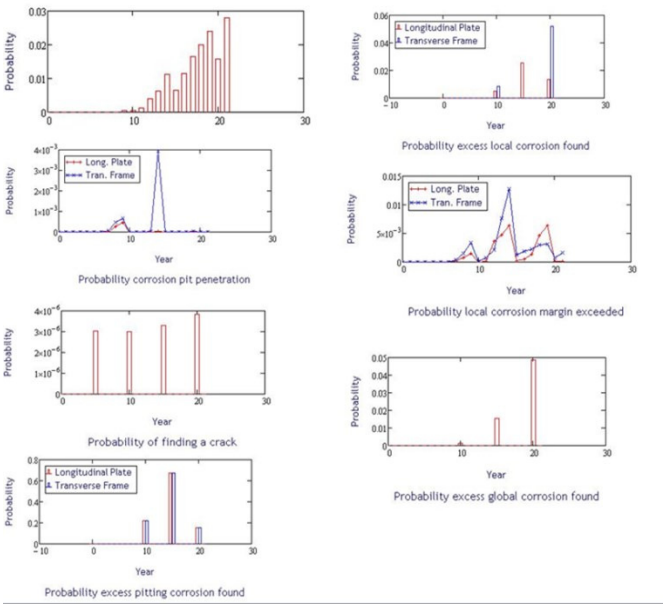

Figure 22 Representative results for Crack C2

This method along was presented as part of the INCASS project ((INCASS 2015a & 2015b)

6 DECISION SUPPORT SOFTWARE

In order to incorporate the results presented in comprehensive software and provide decision support to the user the software tool developed is presented in Figure 23 (INCASS 2015b).

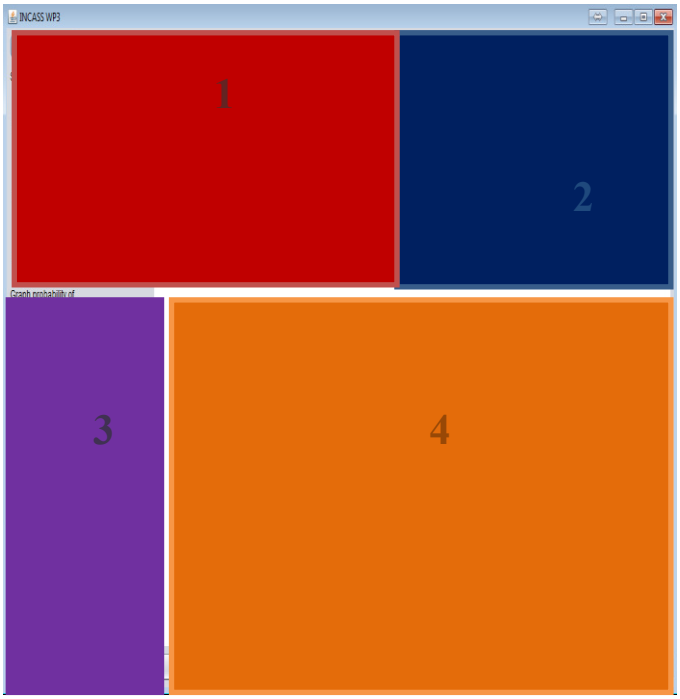

Figure 23 DSS Software tool for structural reliability

The tool is separated into four areas. Starting from the top left (Fig. 23 – 1) the user can specify a location on a selected ship in x, y, z coordinates to be investigated. The top right area (Fig 23 – 2)can be used so that the user introduces new data for analysis and also performs the required analysis through execution of the relevant model. The other two areas at the bottom half of the user interface (Fig 23 – 3,4) provide the user with access in order to investigate the results of the analysis. An example, as presented for the two case studies in the previous section of this paper is given in Figure 24. The graphs are presented in order to assist in decision making.

In that respect, the lists on the bottom left (Fig 23 – 3) allow for the user to choose to review the reliability analysis data relevant to this particular point through graphs presented on the bottom right left (Fig 23 – 4) as in the example in Figure 24. Through this graph for the particular location on the ship structure that there is probability of corrosion pit penetration for the transverse frame at year 13 and corrective action will be necessary so as to remove that risk.

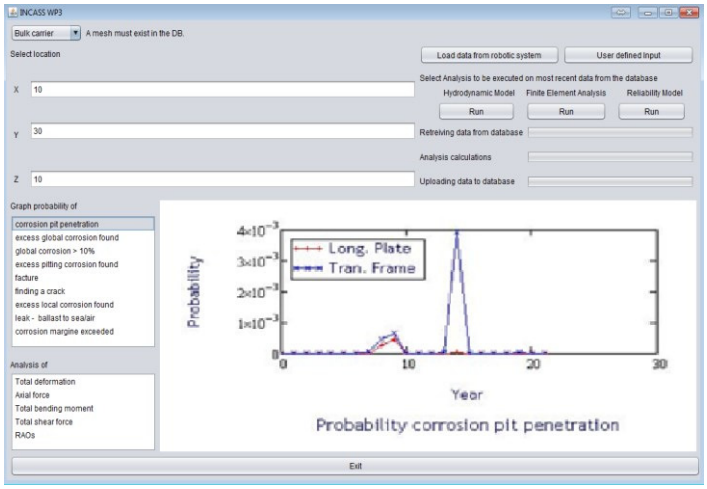

Figure 24 Reliability result presented for Bulk Carrier crack C1

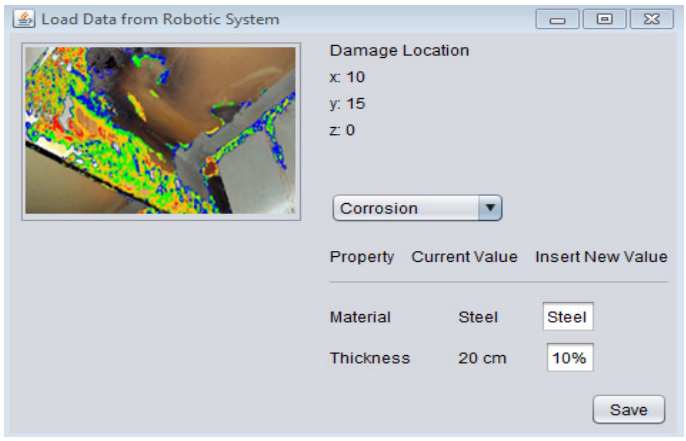

Figure 25 User inspection of robotic data

In order for the user to be able to access the robotic data collected through the inspection assistance hardware presented in the INCASS project the soft-

ware through the Robotic data option of the main user interface allows for review of the images collected and gives the user the capability of altering the data automatically recorded through the robot. As an example Figure 25 demonstrates the menu available to the user when reviewing a corrosion image capture by the robot where the processing of the robotic data identified 10% reduction in thickness of the steel. The user can then alter that to a different percentage if appropriate.

A similar menu is provided for user defined input irrespectively of the data collected through robotically assisted inspection. As a result other inspection data can be manually incorporated to the system in order to make the decision support system more versatile in a variety of scenarios that do not depend on deployment of the hardware presented within the INCASS project.

Upon completion of data upload either through the robotic systems or the user input menus available the execution of the three models is provided through the software so that new reliability analysis data can be calculated and new results provided as demonstrated in Figure 26. In this particular example area 2 of the user interface is demonstrated in execution time (Figure 23 – 2).

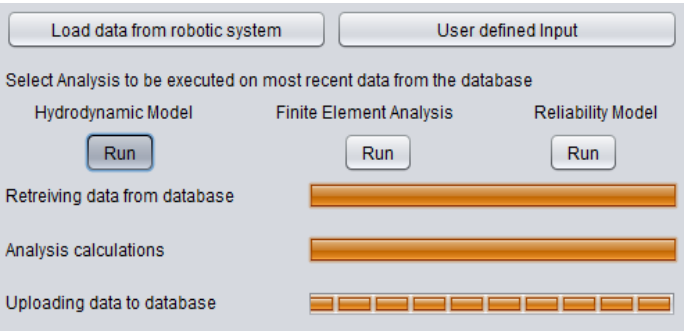

Figure 26 DSS area 2, access to input and model execution

In that respect the software can provide reliability analysis results for any vessel if the appropriate ship historical data is uploaded to the database either through the software or through the database provided interfaces descried within INCASS.

7 CONCLUSIONS

The reliability estimated as a measure of the safety of a structure can be used in a decision process. A lower level of the reliability can be used as a constraint in an optimal design problem. The lower level of the reliability can be obtained by analyzing similar structures designed after current design practice or it can be determined as the reliability level giving the largest utility (benefits – costs) when solving a decision problem where all possible costs and benefits in the expected lifetime of the structural components are taken into account.

In this work environmental, structural data under the light of Bayesian method and structural reliability are combined and capability of incorporating inspection data is develop and failure probability and reliability of critical structural members are calculated which could be applied by the user to enhance structural safety of the vessel.

Moreover, for the data to be presented in a user friendly format a software tool was developed and presented in this work in order to assist in decision making relevant to the structural reliability of the ship. Future work, to make the software more accessible and easier to use, includes replacing the specification of coordinates with a 3D representation of the ship which will be navigated through mouse clicks so that the user can specify points or interest on the structure. Additionally, the areas identified as critical from the analysis results will be highlighted on the 3D structure so that the user can easily identify points requiring maintenance actions which will conclude the DSS software development.

8 ACKWONLEDGEMENTS

INCASS project has received research funding from the European Union's Seventh Framework Program under grant agreement No 605200. This publication reflects only the authors' views and European Union is not liable for any use that may be made of the information contained herein.

REFERENCES

Barltrop, Nigel 2014. Inspection & Survey NM946 Part 3 Marine Materials & Structures NM312 Fatigue and Fracture Part 3.

Choi, Seung-Kyum, Ramana Grandhi, & Robert A Canfield 2006. *Reliability-Based Structural Design*. Springer Science \& Business Media.

DNV 2015. *Probabilistic Methods for Planning of Inspection for Fatigue Cracks in Offshore Structures*.

INCASS 2014a. Deliverable D3.1 Structural life cycle management. *INCASS - Inspection Capabilities for Enhanced Ship Safety. EC FP7 Project*.

INCASS 2014b. Deliverable D3.2 Interface and analysis of data collected by robots. *INCASS - Inspection Capabilities for Enhanced Ship Safety. EC FP7 Project*.

INCASS 2014c. Deliverable D3.3 Hydrodynamic and structural analysis. *INCASS - Inspection Capabilities for Enhanced Ship Safety. EC FP7 Project*.

INCASS 2015a. Deliverable D3.4 Analysis and consolidation of structural data (including real time measurements). *INCASS - Inspection Capabilities for Enhanced Ship Safety. EC FP7 Project.*

INCASS 2015b. Deliverable D3.5 Development of a decision support system for ship structure and emergency decision support system. *INCASS - Inspection Capabilities for Enhanced Ship Safety. EC FP7 Project.*